*Published online 28 September 2022* *Nucleic Acids Research, 2022, Vol. 50, No. 18* ***10785–10800***
*https://doi.org/10.1093/nar/gkac822*

# Functional integration of a semi-synthetic azido-queuosine derivative into translation and a tRNA modification circuit

**Larissa Bessler[1,†], Navpreet Kaur[2,†], Lea-Marie Vogt[1,†], Laurin Flemmich[3], Carmen Siebenaller[4], Marie-Luise Winz[1], Francesca Tuorto[5], Ronald Micura[3], Ann E. Ehrenhofer-Murray[2,*] and Mark Helm[1,*]**

[1]Institute of Pharmaceutical and Biomedical Sciences, Johannes Gutenberg-University Mainz, 55128 Mainz, Germany, [2]Institute of Biology, Humboldt-Universität zu Berlin, 10117 Berlin, Germany, [3]Department of Organic Chemistry, University of Innsbruck, 6020 Innsbruck, Austria, [4]Department of Chemistry – Biochemistry, Johannes Gutenberg-University Mainz, 55128 Mainz, Germany and [5]Division of Biochemistry, Mannheim Institute for Innate Immunoscience (MI3), Medical Faculty Mannheim, Heidelberg University, Mannheim, Germany

Received June 15, 2022; Revised September 09, 2022; Editorial Decision September 09, 2022; Accepted September 27, 2022

## ABSTRACT

**Substitution of the queuine nucleobase precursor preQ$_1$ by an azide-containing derivative (azido-propyl-preQ$_1$) led to incorporation of this clickable chemical entity into tRNA *via* transglycosylation *in vitro* as well as *in vivo* in *Escherichia coli*, *Schizosaccharomyces pombe* and human cells. The resulting semi-synthetic RNA modification, here termed Q-L1, was present in tRNAs on actively translating ribosomes, indicating functional integration into aminoacylation and recruitment to the ribosome. The azide moiety of Q-L1 facilitates analytics *via* click conjugation of a fluorescent dye, or of biotin for affinity purification. Combining the latter with RNAseq showed that TGT maintained its native tRNA substrate specificity in S. *pombe* cells. The semi-synthetic tRNA modification Q-L1 was also functional in tRNA maturation, in effectively replacing the natural queuosine in its stimulation of further modification of tRNA$^{Asp}$ with 5-methylcytosine at position 38 by the tRNA methyltransferase Dnmt2 in *S. pombe*. This is the first demonstrated *in vivo* integration of a synthetic moiety into an RNA modification circuit, where one RNA modification stimulates another. In summary, the scarcity of queuosinylation sites in cellular RNA, makes our synthetic q/Q system a 'minimally invasive' system for placement of a non-natural, clickable nucleobase within the total cellular RNA.**

## INTRODUCTION

Post-transcriptional modification of tRNAs is a ubiquitous yet idiosyncratic feature with versatile chemical structures contributing to stability and folding, as well as fidelity of decoding and translational control (1–3). The largest variety of chemical structures in RNA is found in the anticodon loop which directly interacts with the mRNA during decoding in the translating ribosome. The chemical variety of the more than 170 modifications known to date is dominated by tRNA anticodon modifications occurring at positions 34 and 37, ranging from simple methylations to highly complex structures of which queuosine (Q) is a particular case (4,5). In both, prokaryotes and eukaryotes, this hypermodified 7-deazaguanosine is exclusively found in the anticodon wobble position 34 of tRNAs containing a $G_{34}U_{35}N_{36}$ motif and therefore specific for a selected group of four tRNAs, namely tRNA$^{Asn}$, tRNA$^{Asp}$, tRNA$^{His}$ and tRNA$^{Tyr}$ (6,7). In an intricate multi-step process involving various enzymes and co-factors, *Escherichia coli* and other prokaryotes are capable of first synthesising the modified precursor base 7-aminomethyl-7-deazaguanine (preQ$_1$) *de novo*. GTP is converted to preQ$_1$ *via* five enzymatic steps successively catalysed by the GTP cyclohydrolase I (GCH I), QueD, QueE, QueC and QueF (8–11). As a rare type of post transcriptional modification, the noncanonical nucleobase structure is then introduced into tRNA in an exchange reaction. During this transglycosylation step, the bacterial tRNA guanine transglycosylase (bTGT) replaces

*To whom correspondence should be addressed. Tel: +49 6131 39 25731; Fax: +49 6131 39 20373; Email: mhelm@uni-mainz.de
Correspondence may also be addressed to Ann E. Ehrenhofer-Murray. Tel: +49 30 2093 49630; Fax: +49 30 2093 49641; Email: ann.ehrenhofer-murray@hu-berlin.de
†The authors wish it to be known that, in their opinion, the first three authors should be regarded as Joint First Authors.

a guanosine in the anticodon wobble position of cognate tRNAs with the precursor base $preQ_1$ (12,13) which is then further enzymatically modified by QueA and QueG to yield the final queuosine structure (14,15). In contrast to prokaryotes, eukaryotes salvage the nucleoside queuosine and the corresponding nucleobase queuine (q) from environmental sources including the gut microbiota (reviewed in (5)). Queuosine is hydrolyzed by a queuosine nucleoside glycosylase to release q (16). The incorporation of the salvaged q into tRNA is catalysed by eukaryotic TGT (eTGT), which is a heterodimeric enzyme (17–19) composed of a catalytic queuine tRNA-ribosyltransferase subunit 1 (QTRT1) and a noncatalytic queuine tRNA-ribosyltransferase subunit 2 (QTRT2) (20).

Despite its suggestive positioning at position 34 of the tRNA anticodon, molecular details of the physiological relevance of Q remain scarce. It is generally accepted that Q impacts the decoding process on the translating ribosome, with cumulative evidence pointing to pivotal interactions at the A-site. The specific occurrence of Q in GUN anticodons is consistent with a general concept by Grosjean and Westhof (21), wherein modifications at position 34 compensate for the lower stability of codon-anticodon interactions including 2 or more base pairs with less than three hydrogen bonds. This concept receives support from computational modelling, which characterised a stabilising effect of Q on the overall tRNA-mRNA complex involving additional hydrogen bonds (22). *In vivo* and *in cellulo* studies did not reveal any strong phenotypes under Q deficiency or in strains lacking TGT. However, the presence of Q improved viability under stress conditions and affected translation accuracy in *E. coli* (23,24). *In vivo* studies in eukaryotes likewise reported an impact on the decoding process, enabling decoding of synonymous codons by wobble base pairing (22,25,26), and affecting translation speed and accuracy (27,28). Queuosine's multifaceted involvement in the cellular machinery was reported to be associated with cancer (29–32), neuronal disorders (33–35) as well as bacterial and parasitic infection (36,37). Consequently, the perception of therapeutic potential associated with its biogenesis has consistently increased, in keeping with a general trend in epitranscriptomics

So far, the only demonstrated molecular interaction affected by Q outside the ribosome is a so-called modification circuit with 5-methylcytidine ($m^5C$) in position 38 of *Schizosaccharomyces pombe* $tRNA^{Asp}$, stimulating its formation by the Dnmt2 homologue Pmt1 (38,39). Structural analysis suggested that the presence of Q34 leads to optimal positioning of the interacting substrates in the active site of Dnmt2, enhancing the catalytic efficiency of the methyltransferase (40).

Arguably, approaches to a deeper understanding of the molecular action of Q in living cells would need to involve manipulations of details of the structure of Q, e.g. *via* an incorporation of q-derivatives through transglycosylation. Apart from their natural substrates, both bTGT and eTGT have been shown to tolerate a certain variety of synthetic analogues harbouring large functional groups *in vitro* (41,42). Leveraging the short hairpin recognition motif of the bTGT installed on different RNA transcripts, Devaraj and co-workers developed a method called RNA-TAG (transglycosylation at guanosine), allowing to site-specifically incorporate analogues *in vitro*, which contained large fluorophores or affinity labels for pull-down experiments. This method was also applied to visualize mRNA transcripts containing the recognition motif in a fixed cell environment in a direct one-step-reaction (42) and extended to the development of a light-activated mRNA translation system (43). Furthermore, RNA-TAG was used on modified mRNAs in a two-step-approach, incorporating a $preQ_1$-derivative bearing a bioorthogonal tetrazine moiety in the first step, and thus enabling further derivatization by IEDDA click chemistry in a second step (44). However, labelling with click-competent compounds *in vivo* or *in cellulo* has not yet been achieved in the queuosine field. Indeed, there is strongly suggestive, albeit indirect evidence of successful *in vivo* incorporation of a non-natural q-analogue as published by Kelly and co-workers in the context of an animal model of multiple sclerosis (34). In addition to concerns about cell permeability of a q-derivative, important aspects to determine for *in vivo* labelling studies would include the physiological impact of an artificial chemical structure in a functioning tRNA, which would primarily be expected on the level of translation.

In this study, we metabolically label tRNA with a $preQ_1$ derivative functionalized with an azide group, allowing for further derivatization by click reaction and thus facilitating the proof of successful incorporation as well as the isolation of accordingly tagged RNAs. The latter was combined with RNAseq, in order to re-investigate the RNA substrates of the TGT, which turned out to be specific for the previously reported tRNAs Asn, Asp, His and Tyr. While in previous studies the transglycosylation step was performed in a fixed cell environment, we herein focus on the incorporation of the analogues by the natively expressed TGT *in vivo* and the physiological consequences in the natural environment. Polysome preparations revealed an enrichment of Q-containing tRNAs in the polysomal fraction, indicating a targeted selection for modified tRNA to be integrated in the translational process. Moreover, our data demonstrate that the semi-synthetic tRNA modification replaces Q34 and is functionally integrated into the translational process, as well as in the modification circuit with $m^5C38$ in $tRNA^{Asp}$ in *S. pombe*.

## MATERIALS AND METHODS

*S. pombe* strains used in this study are given in Supplementary Table S1, Plasmids used in this study are given in Supplementary Table S2, oligonucleotides used in this study are given in Supplementary Table S3. The names and versions of all software used are provided in Supplementary Table S4.

### Synthesis of $preQ_1$-L1, $preQ_1$-L2 and $preQ_1$-L3

The $preQ_1$-ligands were synthesized as previously described (45).

### Recombinant expression and purification of bTGT

The pASK-IBA13plus vector expressing the *Zymomonas mobilis* TGT (bTGT) with a N-terminal Strep-tag II was kindly provided by Prof. Dr Klaus Reuter (Philipps-University, Marburg). Expression and purification were carried out as previously described with minor changes (46). Briefly, the TGT was expressed in *E. coli* BL21-CodonPlus (DE3)-RIPL cells, grown in 2× YT medium and protein production was induced using anhydrotetracycline to a final concentration of 0.2 mg/l. After growing the cells for 14 h at 15°C, cells were harvested and the cell pellets were stored at –80°C until further processing. To purify the bacterial TGT, cells were thawed in lysis buffer (100 mM Tris pH 7.8, 150 mM NaCl, 1 mM EDTA pH 8.0, 2 mM PMSF, 1 μg/ml leupeptin, 1 μg/ml aprotinin, 1 μg/ml pepstatin and 25 U of DNase I and RNase I, respectively). After sonication (60% amplitude, 6 min, 0.5 s on, 2 s off; Sonifier 250 D, Branson), soluble proteins were isolated by centrifugation at 20 000 g for 1 h, 4°C. Affinity chromatography was then used to purify the Strep II-tagged TGT. For this purpose, the lysate was incubated with Strep-Tactin® Superflow Plus resin (Qiagen) for 3 h at 4°C, 15 rpm. After washing with washing buffer (100 mM Tris pH 7.8, 150 mM NaCl, 1 mM EDTA pH 8.0), the protein complex was eluted in 100 mM Tris pH 7.8, 150 mM NaCl, 1 mM EDTA pH 8.0 and 2.5 mM desthiobiotin. Further purification was achieved by Superdex S200 (GE Healthcare) size exclusion chromatography (10 mM Tris pH 7.8, 150 mM NaCl, 1 mM EDTA pH 8.0). The purified bTGT was stored at –80°C in 10 mM Tris pH 7.8, 150 mM NaCl, 1 mM EDTA pH 8.0 with 50% glycerol.

### *E. coli* strains and growth conditions

The *E. coli* Keio parent strain (BW25113) and the knockout strains for QueD, QueC, QueE, QueF and TGT were obtained from the *E. coli* Keio knockout collection (GE Healthcare (Dharmacon™), England) and grown in standard M9 medium (6.8 g/l $Na_2HPO_4$, 3 g/l $KH_2PO_4$, 0.5 g NaCl, 1 g/l $NH_4Cl$, 2 mM $MgSO_4$, 0.1 mM $CaCl_2$, 0.4% glucose) at 37°C and 190 rpm. Growth medium of knockout strains was additionally supplemented with kanamycin (25 μg/ml). Synthetic $preQ_1$-derivatives were added to final concentrations of 0.1, 1, 5 or 10 μM to the culture, respectively.

### Isolation of total tRNA from *E. coli*

To isolate total tRNA, *E. coli* cells were grown to an $OD_{600}$ of 1 in 50 ml cultures and harvested by centrifugation (10 min, 10 000 g, 4°C). The RNA was extracted by using the RNA isolation reagent TRI Reagent© (Sigma-Aldrich, Germany) following the manufacturer's instructions and dissolved in MQ-water.

### Polysome preparations from *E. coli*

For polysome preparations the *E. coli* cells were grown in M9 medium in 150 ml culture volume until they reached an OD of 0.6, chloramphenicol was added to final concentration of 100 μg/ml and after further incubation of 3 min the cells were harvested by centrifugation (10 min, 10 000 g, 4°C). For cell lysis, cell pellets were resuspended in buffer (100 mM $NH_4Cl$, 10 mM $MgCl_2$, 20 mM Tris, pH 7.5), lysozyme was added and freeze-thaw cycles in liquid nitrogen were performed. Subsequent to this 10% deoxycholate was added to complete lysis, remaining cell wall debris were separated by centrifugation (12 000 g, 10 min, 4°C). Sucrose gradients from 5 to 40% were generated using a Biocomp gradient station model 108 (settings: time 1.24 min, angle 81.5°, speed 21 rpm) and lysate was loaded on top of the gradient. After ultracentrifugation (Beckman Ultracentrifuge Optima LE-80K, SW40 Ti rotor from Beckman Coulter) at 150 000 g and 4°C for 2.5 h, gradients were fractionated by measuring the absorbance at 280 nm (Biocomp Gradient Station model 108 in combination with Gilson Fraction Collector FC203B). Total RNA was isolated from the respective fractions using TRI reagent© (Sigma-Aldrich).

### Purification of total tRNA from collected fractions by gel elution

Total RNA extracted from polysomal fraction was separated on a 10% denaturing PAGE gel, stained with GelRed (Biotium) and the bands were visualized on Typhoon 9400 at an excitation wavelength of 532 nm. According to the resulting image, bands of interest were excised from the gel and mashed with a scalpel. The mashed gel pieces were frozen for 1 h and 300 μl of 0.5 M ammonium acetate were added. Subsequently, the samples were shaken at 25°C and 750 rpm overnight. The gel suspension was filtered through NanoSep® centrifugal filters and the filtrate was precipitated with three volumes of 100% ethanol.

### *S. pombe* strains, plasmids and growth conditions

The *S. pombe* strains and plasmids used in this study are shown in Supplementary Table S1. Cells were cultured in YES (5 g/l yeast extract, 30 g/l glucose, 250 mg/l adenine, 250 mg/l histidine, 250 mg/l leucine, 250 mg/l uracil, 250 mg/l lysine) which did not contain queuosine or queuine. Synthetic queuine (kindly provided by Hans-Dieter Gerber and Gerhard Klebe (Universität Marburg) (47)) and $preQ_1$ derivatives were added to 0.1 μM to the culture.

### Isolation of total RNA and small RNAs from *S. pombe*

To isolate total RNA, *S. pombe* cells were grown to an optical density at 600 nm ($OD_{600}$) of 1 in 50 ml cultures. 50 OD of cells were harvested and 1 ml of phenol, glass beads were added. After vigorous shaking for 5 min, samples were centrifuged at 20 000 g for 5 min to clear the cell debris. Equal volume of phenol/chloroform/isoamylalcohol was added to the aqueous phase and centrifuged at 20 000 g for 5 min. After mixing the upper phase with an equal volume of chloroform followed by centrifugation at 20 000 g for 5 min, the RNA was precipitated at –80°C for 1 h using 0.7 volume of isopropyl alcohol. Following precipitation, total RNA was washed with 70% ethanol and eluted in DEPC-treated water.

Isolation of small RNAs was performed using the PureLink™ miRNA Isolation Kit (Invitrogen) according to the manufacturer's instructions. Yeast cells were grown to an $OD_{600}$ of 1 in 5 ml cultures. After harvesting 1 OD of cells, RNAs were isolated using 1 ml TriFast reagent (Peqlab), 0.2 ml chloroform and glass beads. After vigorous shaking for 2 min, samples were centrifuged at 16 000 g, 4°C for 15 min. After adding 215 μl ethanol to the aqueous phase, the samples were transferred to a spin cartridge followed by centrifugation at 12 000 g for 1 min. 700 μl ethanol was added to the flow-through and the sample was transferred to a new spin cartridge. Following centrifugation at 12 000 g for 1 min, the cartridge was washed and small RNAs were dissolved in DEPC-treated water. Northern blot–acryloyl aminophenylboronic acid (APB) gels were performed as previously described (28).

### Removal of ribosomal RNA

Depletion of ribosomal RNA was performed as previously described (48). Oligonucleotides specific for 5.8S and 5S rRNA were ordered with a 5'-biotin tag from Metabion (see Supplementary Table S3). The oligonucleotides were diluted to 100 μM each in nuclease-free water and equal volumes of the 100 μM stock were combined to generate the rRNA depletion mix.

For hybridization, 8 μg of small RNAs were incubated with 9.92 μl of the 100 μM rRNA depletion mix in reaction buffer (10 μl of formamide, 2.5 μl of 20× SSC (3 M NaCl, 0.3 M sodium citrate, pH 7.0) and 5 μl of 0.005 M EDTA, pHnbsp;8). Reactions were carried out in a total volume of 50 μl with the following thermocycling: 80°C for 5 min, ramp down to 25°C at intervals of 5°C per minute. Following hybridization, 2 μl of RNase-OUT (Invitrogen) and 50 μl of 1× SCC containing 20% formamide were added. Removal of rRNA/oligonucleotide hybrids was performed using Dynabeads™ MyOne™ Streptavidin C1 (ThermoFisher) according to the manufacturer's instructions. 500 μl streptavidin coated magnetic beads were washed as instructed for immunoprecipitation of RNA and added to the hybridization reaction. After incubation for 15 min at room temperature with mild agitation and bead separation on a magnetic rack, the supernatant was once more incubated with 500 μl of washed beads for 15 min at room temperature under mild agitation followed by bead separation. Subsequently, the supernatant containing the 5S/5.8S rRNA-depleted RNA was precipitated with 1/10 volume of ammonium acetate and three volumes of 100% ethanol.

### RNA substrates for *in vitro* modification

The *S. pombe* $tRNA^{Asp}$ substrate was prepared as previously described (49). Briefly, the pJET1 vector carrying the $tRNA^{Asp}$ sequence was linearized with NcoI, and 2.5 μg of the linear vector was used for *in vitro* transcription using the TranscriptAid T7 High Yield Transcription Kit (Thermo Fisher Scientific) according to the manufacturer's instructions. Following an 8 h incubation at 37°C with nucleotides and the T7 RNA polymerase and subsequent DNase I treatment, the respective tRNA was purified from the reaction using phenol/chloroform extraction followed by gel filtration with Sephadex G50 (GE Healthcare).

### Recombinant expression and purification of hTGT

The pCDF-Duet1 vector co-expressing the human TGT (hTGT) heterodimer QTRT1 and QTRT2 with a cleavable N-terminal 6xHis tag to QTRT1 was kindly provided by Prof. Dr. Ralf Ficner (GZMB, Göttingen). Expression and purification were carried out as previously described with minor changes (20). Briefly, the heterodimer QTRT1/QTRT2 was co-expressed in *E. coli* (DE3) Rosetta cells, and protein production was induced using autoinduction. After growing the cells for 50 h at 18°C, cells were harvested and the cell pellets were stored at –80°C until further processing. To purify the human TGT, cells were thawed in lysis buffer (50 mM HEPES pH 7.5, 100 mM NaCl, 10 mM imidazole, 2 mM PMSF, 1 μg/ml leupeptin, 1 μg/ml aprotinin, 1 μg/ml pepstatin and 25 U of DNase I and RNase I, respectively). After sonification (60% amplitude, 6 min, 0.5 s on, 2 s off; Sonifier 250 D, Branson), soluble proteins were isolated by centrifugation at 20 000 g for 1 h. Affinity chromatography was then used to purify the 6xHis tagged QTRT1/QTRT2 complex. For this purpose, the lysate was incubated with Talon® Superflow™ resin (Cytiva) for 3 h at 4°C, 15 rpm. After washing with washing buffer (50 mM HEPES pH 7.5, 100 mM NaCl, 10 mM imidazole and 1 M LiCl), the protein complex was eluted in 50 mM HEPES pH 7.5, 100 mM NaCl and 500 mM imidazole. Further purification was achieved by Superdex S200 (GE Healthcare) size exclusion chromatography (20 mM HEPES pH 7.5, 100 mM NaCl). The purified hTGT was stored at –80°C in 20 mM HEPES pH 7.5, 100 mM NaCl with 50% glycerol.

### *In vitro* labelling of tRNA with $preQ_1$ derivatives

For *in vitro* labelling of tRNA with the $preQ_1$ derivatives, 10 μM of *in vitro* transcribed tRNAs or alternatively 10 μg of total RNA from *S. pombe* was incubated with 200 nM hTGT (QTRT1:QTRT2) and 5 μM queuine in reaction buffer (50 mM Tris–HCl pH 7.5, 20 mM NaCl, 5 mM $MgCl_2$ and 2 mM dithiothreitol) for 5 h at 37°C. The RNA was purified using phenol/chloroform extraction and precipitated with 1/10 volume of ammonium acetate and three volumes of 100% ethanol.

### HeLa cells growth conditions and *in vivo* labelling with $preQ_1$-L1

HeLa cell lines were obtained from ATCC and authenticated by multiplex human cell line authentication test (Multiplexon). Cells were grown in Dulbecco's modified Eagle's medium (DMEM) (Thermo Fisher Scientific). The cultures were supplemented with 10% heat-inactivated FBS, 2 mM L-glutamine and a commercial cocktail of antibiotics (Thermo Fisher Scientific). For minus-Q conditions, ultraculture serum-free medium (Lonza) was supplemented with 2 mM L-glutamine and 100 units/ml Penicillin/Streptomycin. $preQ_1$-L1 derivative was added at a concentration of 0.1 μM for 72 h to the culture.

### HeLa cell polysome profiling

$10^7$ cells were treated with 100 μg/ml cycloheximide for 5 min at RT to stabilize existing polysomes before washing with ice-cold PBS and harvesting by scraping in 400 μl polysome lysis buffer (20 mM Tris–HCl, pH 7.4, 5 mM $MgCl_2$, 150 mM NaCl, 1 mM DTT, 1% Triton X-100, 100 μg/ml cycloheximide, 1 × Complete Protease Inhibitors (Roche)). Lysates were rotated end-over-end for 10 min at 4°C and cleared by at 10 000 rpm for 10 min at 4°C. 40 μl of supernatant lysate was saved as input before loading the lysates to linear 17.5 to 50% sucrose gradients in 20 mM Tris–HCl (pH 7.4), 5 mM $MgCl_2$, 150 mM NaCl. Centrifugation was carried out at 35 000 rpm for 2.5 h at 4°C in a Beckmann SW60 rotor. Gradients were eluted with an ISCO UA-6 gradient fractionator, and polysome profiles were recorded by continuously monitoring the absorbance at 254 nm using PeakTrak software. During gradient elution, fractions of ∼300 μl were collected every 14 s. For RNA isolation, 300 μl urea buffer (10 mM Tris, pH 7.5, 350 mM NaCl, 10 mM EDTA, 1% SDS, and 7 M urea) and 300 μl phenol:chloroform:isoamylalcohol (25:24:1) were added to each fraction. After phase separation, RNA was isolated from the aqueous phase and precipitated using isopropanol and GlycoBlue (Thermo Fisher Scientific).

### CuAAC click reaction

Chemical clicking was performed as previously described (50). Briefly, up to 10 μg of RNA was incubated in reaction buffer containing 50% (v/v) DMSO, 5 mM Tris ((1-hydroxy-propyl-1*H*-1,2,3-triazol-4-yl)methyl) amine (THPTA), 5 mM sodium ascorbate, 0.5 mM $CuSO_4$ and 50 μM ligand alkyne under light-protection for 2 h at 25°C. The ligand alkynes used were AlexaFluor 594 alkyne (Thermo Fisher Scientific) or biotin alkyne (PEG4 carboxamide-Propargyl biotin; Thermo Fisher Scientific). RNA was precipitated with 1/10 volume of ammonium acetate and three volumes of 100% ethanol.

### Detection of queuine and preQ$_1$ modification of RNAs

Labelled RNA that had been CuAAC-clicked with AlexaFluor 594 alkyne was analyzed by denaturing PAGE. Up to 10 μg of labelled RNA was separated in 10% polyacrylamide gels (acrylamide/ bisacrylamide (19:1), urea 8 M in 1× TBE buffer). Detection was carried out on the Typhoon 9500 (GE Healthcare) using 532 nm for excitation. As a loading control, gels were stained with Sybr Gold nucleic acid gel stain (Thermo Fisher Scientific) or GelRed (Biotium) for 10 min followed by detection using 495 or 532 nm, respectively, for excitation.

To detect the queuine modification, 300 ng of total RNA or small RNAs from *S. pombe* WT and *qtr2Δ* strains were separated in a 10% polyacrylamide gel (acrylamide/ bisacrylamide (19:1), urea 8 M) supplemented with 5 mg/ml 3-(acrylamido)-phenylboronic acid as described previously (51). The separation was performed at room temperature in 1× TBE. The electrophoresed gels were transferred to a Biodyne B Nylon membrane (0.45 μM). Selected RNAs were detected using a 5′-biotin-labeled probe at a final concentration of 0.3 μM and the Chemiluminescence Nucleic Acid Detection Module Kit (Thermo Fisher Scientific) according to the manufacturer's instructions. The first blocking step was carried out using the DIG Easy Hyb buffer (Roche), and hybridization was performed overnight at 45°C.

### Detection of Q and Q-L1 by LC–MS/MS analysis

Up to 5 μg of total tRNA was digested to nucleoside level using 0.6 U nuclease P1 from *P. citrinum* (Sigma-Aldrich), 0.2 U snake venom phosphodiesterase from *C. adamanteus* (Worthington), 2 U FastAP (Thermo Fisher Scientific), 10 U benzonase (Sigma-Aldrich), 200 ng Pentostatin (Sigma-Aldrich) and 500 ng Tetrahydrouridine (Merck-Millipore) in 25 mM ammonium acetate (pH 7.5; Sigma-Aldrich) overnight at 37°C. 1 μg of total tRNA was analyzed *via* LC–MS using an Agilent 1260 series LC with a Synergi Fusion column (4 μM particle size, 80 Å pore size, 250 × 2.0 mM; Phenomenex) and an Agilent 6460 Triple Quadrupole mass spectrometer equipped with an electrospray ion source (ESI). The elution started with 100% solvent A (5 mM ammonium acetate buffer, pH 5.3) with a flow rate of 0.35 ml/min at 35°C, followed by a linear gradient to 8% solvent B (LC–MS grade acetonitrile; Honeywell) at 10 min and 40% solvent B after 20 min. Initial conditions were regenerated with 100% solvent A for 10 min. The UV signal at 254 nm was recorded *via* a multiple wavelength detector (MWD) detector at 254 nm to monitor the main nucleosides. The following ESI parameters were defined for the measurement: gas temperature 350°C, gas flow 8 l/min, nebulizer pressure 50 psi, sheath gas temperature 350°C, sheath gas flow 12 l/min, capillary voltage 3000 V, nozzle voltage 0 V. The MS was operated in the positive ion mode using Agilent MassHunter software in the dynamic MRM (multiple reaction monitoring) mode.

### Identification of preQ$_1$-L1-modified RNAs by HTS

Metabolically labelled and biotin-clicked RNA was purified from total RNA or isolated small RNAs using Dynabeads™ MyOne™ Streptavidin C1 (Thermo Fisher Scientific) according to the manufacturer's instructions. Streptavidin coated magnetic beads were washed as instructed for immunoprecipitation of RNA. 20 μg of biotin-labelled RNA was incubated with the beads for 1 h at room temperature with light agitation. After washing the beads, they were resuspended in nuclease-free water, and bound RNA was dissolved from the beads by incubating the samples at 95°C for 10 min. Library preparation of immunoprecipitated RNAs for deep sequencing was done using the NEBNext Small RNA Library Prep Set for Illumina (Multiplex Compatible; New England Biolabs). 300 ng of RNA per library as starting material was used, and ligation was performed with undiluted adaptors. Adaptor-ligated cDNA was amplified with 15 cycles of PCR reaction using barcoded primers and purified using the Monarch PCR & DNA Cleanup Kit (5 μg) (New England Biolabs). Libraries were eluted in nuclease-free water, multiplexed in equimolar ratios and sequenced on one lane of the Illumina MiSeq platform using paired-end 150 bp sequencing.

### RT-qPCR quantification of tRNA$^{Asp}$, snoR38 and snoR69

For quantification of preQ$_1$-L1-labelled tRNA$^{Asp}$, snoR38 and snoR69 from metabolically labelled and immunoprecipitated (IPed) RNAs, quantitative RT-PCR was performed using a stem-loop primer (see Supplementary Table S3). cDNA was synthesized using IPed RNAs from *S. pombe* WT and *qtr2Δ* and a sequence specific stem-loop primer. First strand synthesis was carried out using the SuperScript™ III First-Strand Synthesis System (Invitrogen) according to the manufacturer's protocol. Synthesized cDNA was subsequently used for qPCR using the PerfeCTa SYBR Green SuperMix (QuantaBio). 4 µl of cDNA was used in a reaction mix containing 12.5 µl Master Mix (Quanta, 2×) and 250 nm primers. Reactions were carried out in a total volume of 25 µl with the following thermocycling: 95°C for 2 min, followed by 40 cycles of 95°C for 10 s, 58°C for 15 s and 72°C for 20 s.

### RNA bisulfite sequencing

Bisulfite sequencing of tRNA$^{Asp}$ was performed as previously described (38). Briefly, bisulfite-treated tRNAs were reverse transcribed using tRNA$^{Asp}$ 3'-specific stem-loop primer followed by amplification with primers binding only to the deaminated sequence at their 5' end. Primer sequences are listed in Supplementary Table S3. Library preparation of the PCR products was performed with the NEXTflex$^{R}$ qRNA-Seq™ Kit v2—Set C (Bioo Scientific) according to the manufacturer's instructions and sequenced on a MiSeq platform using paired-end 150 bp sequencing. Reads were processed using in-house R scripting and the Bioconductor package ShortRead (52). Following the processing, including trimming of PCR primers, selection of high-quality reads and sorting of the reads based on the sequence in the degenerate region of the RT-primer, the reads were analyzed for bisulfite conversion using BISMA (53).

### HTS data processing

The sequencing data was adapter-trimmed using Skewer version 0.2.2 (54) and aligned to *S. pombe* non-coding RNAs (main and mitochondrial) excluding rRNA sequences from Pombase (https://www.pombase.org/) using Salmon version 14.0 (55) and HISAT2 version 2.1.1 (56), as a splice-site sensitive alignment program. The conversion of sam to bam files was performed using SAMtools (57). Aligned sequences were analyzed using custom R scripts and the Bioconductor package DESeq2 (58). Parameters were set to analyze only regions with a minimum of 10 reads and the adjusted *P*-value was set to <0.1. Additionally, independent hypothesis weighting was conducted using the Bioconductor package IHW (59,60) with an adjusted *P*-value of <0.1. Furthermore, peak calling was performed using the Bioconductor package exomePeak2 (61). Plots were generated using the integrative genomics viewer version 2.11.1 (IGV) (62).

## RESULTS

### *In vitro* incorporation of synthetic preQ$_1$ analogues in prokaryotes

To assess the substrate properties of synthetic preQ$_1$-ligands, their incorporation into tRNA by bacterial TGT (bTGT) was tested *in vitro* (Figure 1). For this purpose, preQ$_1$-ligands 1–3 (preQ$_1$-L1-3, Figure 1A), each harbouring an azide group, were incubated with tRNA$^{Asp}$ in the presence of recombinant bTGT from *Z. mobilis*. Taking advantage of the terminal azide group, the successful *in vitro* incorporation of preQ$_1$-ligands was visualized by copper(I)-catalyzed azide alkyne cycloaddition (CuAAC) click reaction of tRNA$^{Asp}$ with the fluorescent AlexaFluor 594-alkyne in the presence of $CuSO_4$, sodium ascorbate and THPTA (tris-((1-benzyl-1*H*-1,2,3-triazol-4-yl)methyl)amine) (Figure 1B and Supplementary Figure S1). As shown by fluorescence scan, all of the tested preQ$_1$-ligands were incorporated to the same extent (Figure 1C), indicating that the side chains attached to the preQ$_1$ structure do not hinder the recognition and turnover by bTGT. This indicates a tolerance of the bTGT active site for large ligands, similar to what was previously described for eTGT *in vitro* (42).

### *In vivo* incorporation of synthetic preQ$_1$ analogues in prokaryotes

After the successful *in vitro* application of synthetic preQ$_1$-ligands with bTGT, we proceeded to metabolic labelling of RNAs *in vivo* in *E. coli*. First experiments were performed with the smallest preQ$_1$ ligand in the series, i.e. preQ$_1$-L1. In a feeding experiment, where an *E. coli* wild-type (WT) strain was grown in medium supplemented with preQ$_1$-L1, total tRNA was isolated and enzymatically digested to the nucleoside level for separation on an RP-C18 HPLC column and subsequent analysis of the Q levels by MS/MS. Of note, queuosine exhibits a fragmentation pattern differing from the standard nucleosides. Instead of the exclusive fragmentation at the *N*-glycosidic bond, cleavage of the ribose in combination with cleavage of the amino linker with a mass shift *m/z* 410 to *m/z* 163 was determined as the most abundant product ion (Supplementary Figure S2a) eluting at a retention time of 12.2 min in the WT sample. Using a fragmentation pattern for the incorporated synthetic nucleoside (Q-L1) that was inferred from that of native queuosine, additional signals for the expected transitions were detected at 16.9 min (Figure 2). Since the product ion *m/z* 163 was the most prevalent species, it was chosen as diagnostic ion in subsequent LC–MS/MS experiments. Monitoring this product ion produced a strong signal for queuosine and only a weak signal for Q-L1 (Supplementary Figure S3c). We concluded that preQ$_1$-L1 was indeed incorporated, but also that it was a weak competitor against the endogenous bacterial preQ$_1$. Consequently, we reasoned that abrogating preQ$_1$ biosynthesis would facilitate the incorporation of the supplied preQ$_1$-ligands. Considering the various steps of Q *de novo* synthesis in *E. coli* (Figure 2A), four different gene deletions, namely *ΔqueD*, *ΔqueE*, *ΔqueC* and *ΔqueF*, were tested for generation of preQ$_1$ by monitoring the presence of

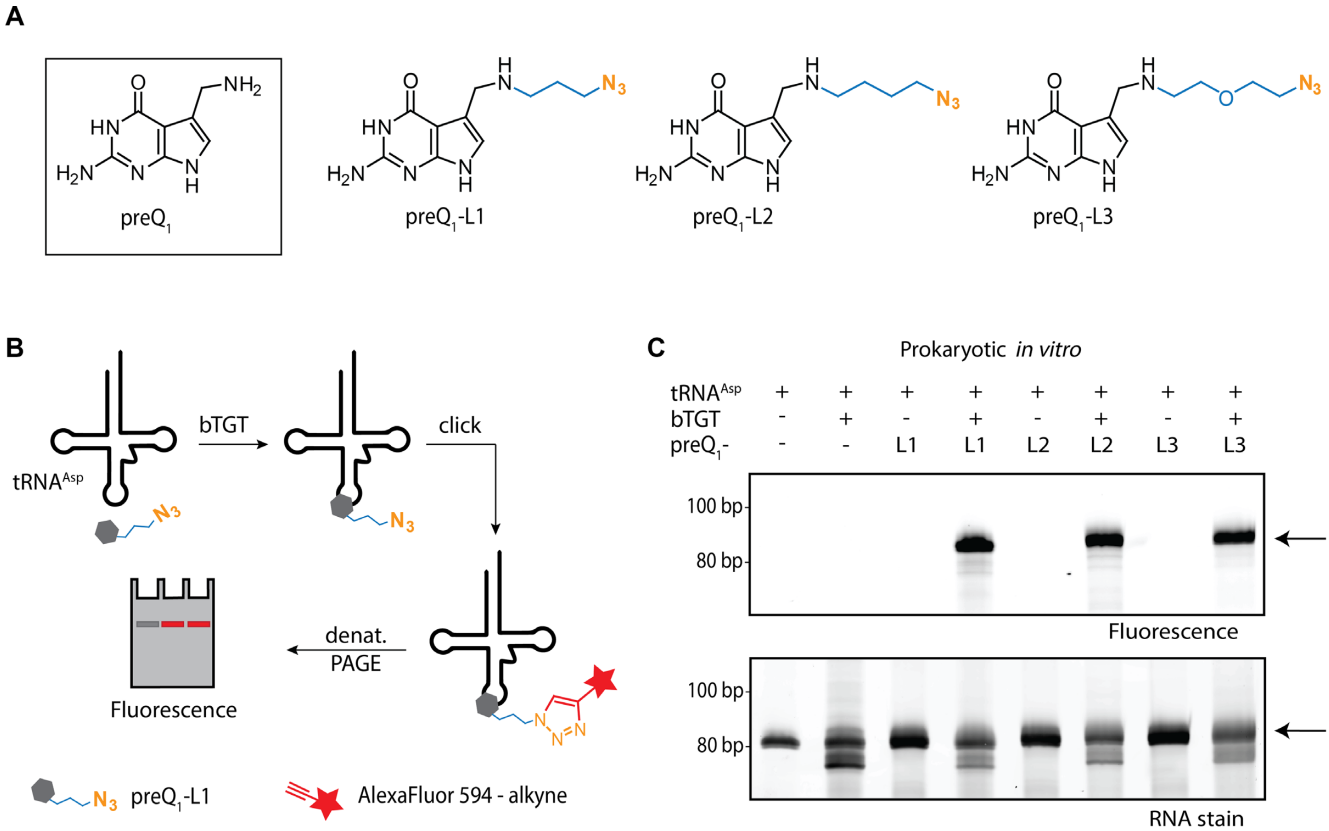


**Figure 1.** *In vitro* incorporation of preQ$_1$ analogues in tRNA$^{Asp}$. (**A**) Natural preQ$_1$ and synthetic preQ$_1$-ligands 1 (L1, 3-azidopropyl-preQ$_1$), 2 (L2, 4-azidobutyl-preQ$_1$) and 3 (L3, 2-(2-azidoethoxy)ethyl-preQ$_1$) containing side chains of different length and constitution (blue) but identical terminal azide groups (orange) designated for click chemistry. (**B**) Scheme of the *in vitro* experiment: incubation of tRNA$^{Asp}$ with preQ$_1$ ligands (exemplarily shown for preQ$_1$-L1) in the presence of bacterial TGT (bTGT) and subsequent click reaction with AlexaFluor 594-alkyne (red), allowing the detection of tRNA with incorporated preQ$_1$ ligand *via* fluorescence scan. (**C**) Analysis of the tRNA$^{Asp}$ click product after bTGT-catalysed incorporation of preQ$_1$-ligands L1–L3 by denaturing PAGE and following visualization by fluorescence scan for AlexaFluor 594 (excitation: 532 nm, emission: 610 nm). A loading control was obtained by RNA staining with GelRed. In both scans, tRNA$^{Asp}$ is indicated by an arrow. Untreated tRNA$^{Asp}$ and tRNA$^{Asp}$ incubated with bTGT or preQ$_1$-ligands L1–L3, respectively, served as controls.

Q at position 34 of tRNAs. The deletion strains showed no significant growth defects compared to the wild type (Figure 2C). To validate the absence of Q *de novo* biosynthesis, tRNA was isolated and analyzed by LC–MS as before; none of the deletion strains generated measurable levels of Q (Supplementary Figure S2b–e). Since all deletions were on a par regarding growth and absence of Q in the isolated total tRNA, *ΔqueD* was chosen for further experiments, given that the absence of QueD prevents *de novo* synthesis of Q in its earliest stages and avoids synthesis of any precursor form (e.g. preQ$_0$ in *ΔqueF*) that was reported to be incorporated by the TGT and might thus compete with preQ$_1$-L1 (Supplementary Figure S3c) (13).

To determine a suitable feeding concentration, the *ΔqueD* cells were supplemented with increasing amounts of preQ$_1$-L1 (Figure 2B), which did not impair the bacterial growth compared to the control without preQ$_1$-L1 feeding (Supplementary Figure S3b). Total tRNA isolated from thus treated *ΔqueD* cells was labelled *via* CuAAC click chemistry and subsequently analysed by denaturing urea PAGE. The fluorescence scan revealed clearly visible fluorescent bands after feeding with preQ$_1$-L1 in a dose-dependent manner, providing evidence for the enzymatic incorporation of the analogue into *E. coli* tRNA *in vivo* (Figure 2D). The signal intensity was quantified using ImageJ software and plotted against the feeding concentration of preQ$_1$-L1 (Figure 2E). To validate these observations, total tRNA isolated from the *ΔqueD* strain treated with preQ$_1$-L1 was further analysed *via* LC–MS/MS. The MS-based analysis of total tRNA isolated from the *ΔqueD* fed with increasing concentrations of preQ$_1$-L1 (0.1–10 μM) confirmed the results obtained from denaturing urea PAGE analysis and related quantification of the fluorescence signal (Figure 2E). Both plots indicate a beginning saturation around 10 μM. Based on the above, a ligand concentration of 5 μM for further feeding experiments was identified as a viable compromise between ligand material consumption and labelling efficiency. Supplementation of a *Δtgt* strain with the optimized concentration of 5 μM preQ$_1$-L1 resulted in no signal for Q-L1 in LC–MS/MS measurements, thus confirming that the incorporation was catalysed by bTGT (Supplementary Figure S3c).

Since preQ$_1$-L1 was successfully incorporated into RNA in bacteria, the *in vivo* experiments were expanded to preQ$_1$-L2 and preQ$_1$-L3. However, in contrast to the previously

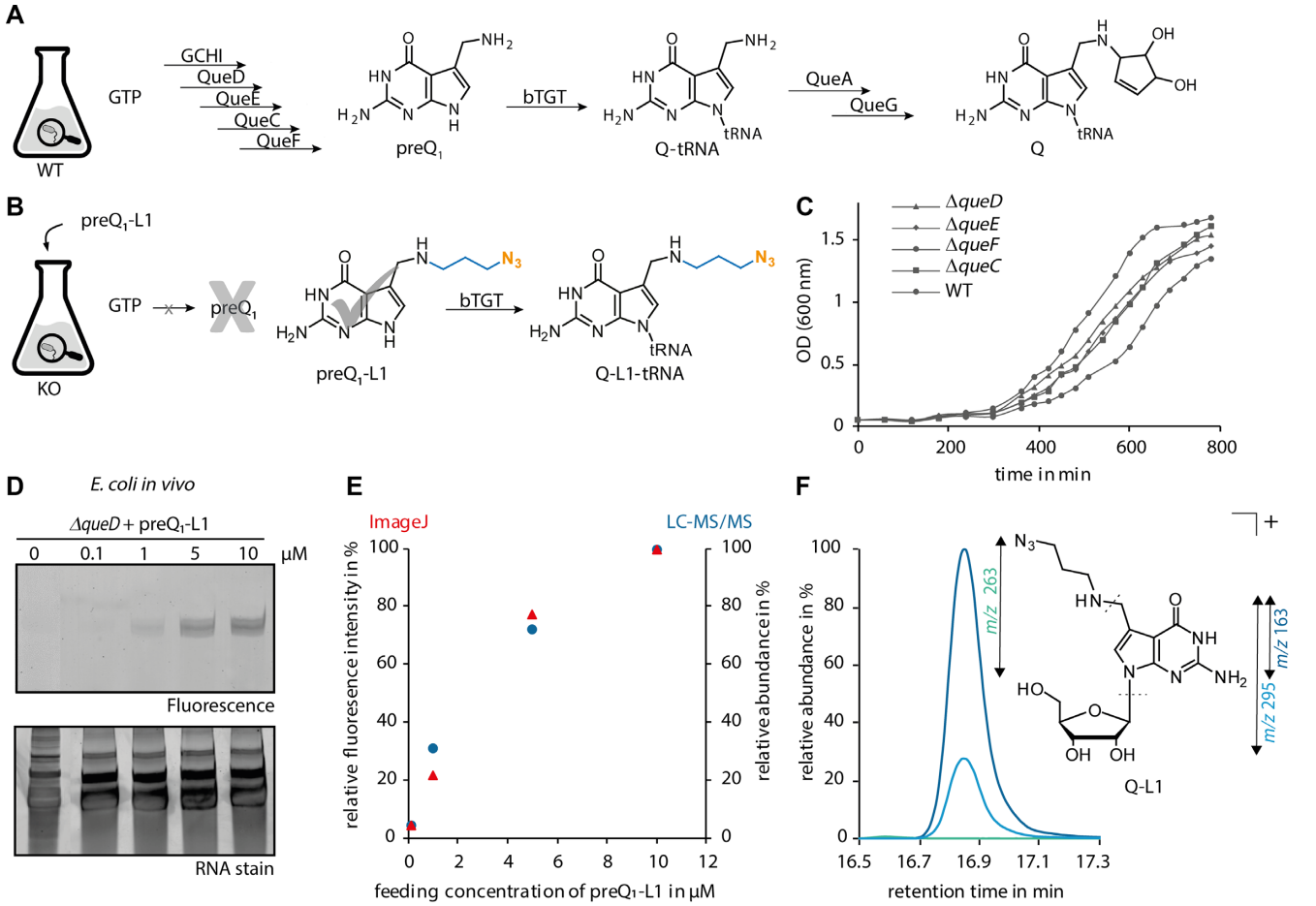


**Figure 2.** *De novo* biosynthesis of Q and induced incorporation of preQ$_1$-L1 in bacteria. (**A**) Biosynthesis of Q in position 34 of tRNAs (Q34-tRNA) *via* insertion of preQ$_1$ into tRNA, which is catalysed by the bacterial tRNA guanine transglycosylase (bTGT). (**B**) Treatment of *E. coli* mutant cells unable to synthesize preQ$_1$ with preQ$_1$-L1 and concomitant bTGT-catalysed incorporation of this analogue into tRNA. (**C**) Growth of the *E. coli* wild-type (WT) strain compared to the growth of several strains with deletions in genes encoding enzymes for Q *de novo* synthesis. (**D**) Analysis of total tRNA from *ΔqueD* cells grown with the indicated concentrations of preQ$_1$-L1 after click reaction by denaturing PAGE and subsequent scanning for fluorescence of AlexaFluor 594 (excitation: 532 nm, emission: 610 nm). (**E**) Merged diagram displaying the quantification of the dose-dependent fluorescence signal obtained from (D) by ImageJ software (Wayne Rasband, NIH) (shown as red triangles) and relative quantification of Q-L1 levels by LC–MS/MS (blue dots). Peak areas of Q-L1 (*m/z* 163) were normalized to the UV signal of adenosine and set in relation to the peak area of the highest feeding concentration (10 μM). (**F**) Extracted ion chromatograms displaying the fragmentation pattern of the incorporated synthetic nucleoside Q-L1 (*m/z* 395) in LC–MS/MS experiments, normalized to the highest peak area (*m/z* 163). Product ions are assigned in the structure of Q-L1.

described *in vitro* experiments, neither feeding preQ$_1$-L2 nor preQ$_1$-L3 at the optimized concentration of 5 μM or at higher concentrations (10 μM for preQ$_1$-L2 and 20 μM preQ$_1$-L3) led to a clear fluorescence signal in the clicked total tRNA samples (Supplementary Figure S3a), indicating that the incorporation efficiency of preQ$_1$-L2 and preQ$_1$-L3 into tRNA *in vivo* was drastically lower compared to preQ$_1$-L1. Since the *in vitro* results indicate indifference of the TGT enzyme towards the alkyl-modified preQ$_1$-ligands, the low incorporation *in vivo* suggests lower bioavailability of preQ$_1$-L2 and preQ$_1$-L3 for the bacteria.

### *In vivo* interactions of synthetic preQ$_1$ analogues in prokaryotes

To investigate possible changes in the ensemble of molecular interactions undergone by Q-L1-carrying tRNA under physiological conditions, we turned to the analysis of polysomes. Given that these consist of actively translating ribosomes, their components, including tRNA, can be considered functional in interactions with essential molecular factors involved in translation. We thus aimed at determining the ratio of Q-L1-carrying tRNAs from polysomes versus that in the remainder of tRNAs.

For this purpose, cell lysates from *E. coli* WT and *ΔqueD* cells supplemented with 10 μM preQ$_1$-L1 were applied to a sucrose gradient (5–40%), enabling the separation of different fractions according to their size after ultracentrifugation. As schematically shown in Figure 3A, free RNAs including tRNAs and some mRNAs were located in fraction F0 at the top of the gradient (5% sucrose), while polysomes accumulated in fraction F3 at a sucrose concentration of ∼40%. This separation was monitored by UV absorbance at 260 nm, and the different fractions were collected. Subsequent to fractionation, total RNA was extracted from these fractions and applied to denaturing PAGE for purification of tRNA *via* gel elution. Digested tRNA samples were subjected to LC–MS/MS

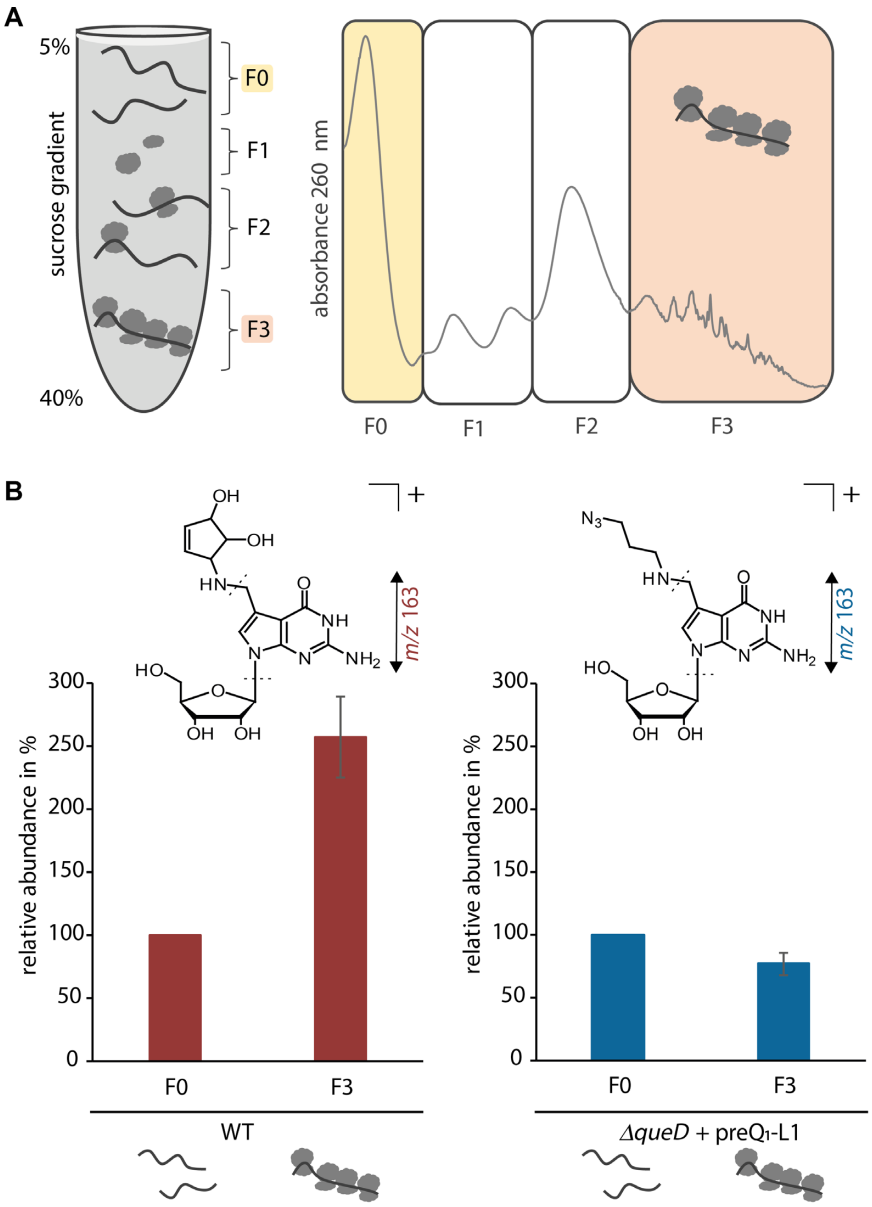


**Figure 3.** *E. coli* polysome preparation and analysis of isolated tRNA obtained from these samples by LC–MS/MS. (**A**) Schematic distribution of fractions F0-F3 from a cell lysate after sucrose gradient (5–40 %) fractionation and ultracentrifugation and representative UV trace at 260 nm (representing RNA) across the sucrose gradient. (**B**) Relative quantification of Q ($m/z$ 410 → 163, red) and Q-L1 ($m/z$ 395 → 163, blue) in tRNA purified from fractions F0 and F3 of WT and *ΔqueD* cells supplemented with 10 μM preQ$_1$-L1 *via* LC–MS/MS. Peak areas were normalized to the UV signal of adenosine and related pairwise to the respective F0 fraction which was set to 100%. The average of normalized and related fractions F0 and F3 of three independent biological replicates are shown.

analysis, and the respective abundances of Q and Q-L1 were compared between the free RNA fraction F0 and the polysomal fraction F3 (Figure 3B). Interestingly, in WT cells, endogenous Q was more abundant in tRNAs isolated from the polysomal fraction compared to fraction F0. This suggests that queuosinylated tRNAs are selectively enriched in polysomes that are actively engaged in translation.

In contrast, the Q-L1 level in polysomal tRNA (F3 fraction) from preQ$_1$-L1 fed *ΔqueD* cells reached a similar amount compared to its level in the respective F0 fraction. This may reflect either a deficit in the aforementioned selection, or a cumulation of minor detrimental effects at the different steps of translation. However, the data clearly illustrate that Q-L1-containing tRNAs actively engage in protein biosynthesis and are able to sustain it at a high enough level to not cause any perceivable growth phenotype.

### *In vitro* incorporation of synthetic preQ$_1$ analogues in eukaryotes

In a next step, the investigations were extended from bacteria to eukaryotes. Of note, eukaryotes do not possess the enzymes to synthesize queuosine *de novo,* but salvage it from external sources for incorporation into tRNA (16). *S. pombe* is a particularly well-suited single cell eukaryotic

model organism, because salient features of queuosine have already been elaborated in this yeast, and queuosine levels can easily be manipulated by supplementation of the growth medium with queuine (38).

We next tested the ability of eTGT to incorporate the preQ$_1$-ligands into RNA *in vitro*. As substrates for this reaction, total RNA was isolated from *S. pombe* wild-type cells or *qtr2Δ* cells cultured in the presence of queuine. In WT cells, this results in Q-modification of the tRNAs, whereas *qtr2Δ* cells lack the essential Qtr2 subunit of *S. pombe* eTGT, therefore maintaining a guanosine in position 34 of the respective tRNAs. Total RNA preparations of these strains were incubated with the preQ$_1$ ligands in presence of hTGT, and subsequently labelled by click reaction. The incorporation of all three ligands into tRNA from both *S. pombe* strains was measured by fluorescence scan (Figure 4A and Supplementary Figure S4b). In comparison to the fluorescence signals of the tRNA from WT cells, the respective signals of the *qtr2Δ* tRNAs showed significantly higher intensities. This indicates that more tRNAs unmodified at position G34 are available for *in vitro* modification with preQ$_1$-L1 in the *qtr2Δ* sample. In contrast, in WT cells only guanosines that were not replaced by Q despite the presence of a functional enzyme remained for the *in vitro* reaction. Unlike observed for the bTGT, the hTGT incorporated the preQ$_1$-ligands to differing degrees, indicating a higher ability to distinguish between these analogues in accordance with previously published results by Kelly and co-workers (41). Additionally, incubation of *in vitro* transcribed tRNAs Asp, His, Tyr and Asn with human TGT and preQ$_1$-L1 showed successful incorporation of the analogue into all of the four tRNAs (Supplementary Figure S4a).

### *In vivo* incorporation of synthetic preQ$_1$ analogues in eukaryotes

Subsequent to the successful *in vitro* experiment, the *in vivo* incorporation of the synthetic preQ$_1$ analogues was examined in *S. pombe*. To this end, *S. pombe* WT and *qtr2Δ* cells (as a control), were cultured in the presence of preQ$_1$-ligands in medium that otherwise lacked Q or q, and RNA was isolated and analysed as before. After click reaction, a fluorescence signal was detected in the RNA isolated from the WT cells treated with preQ$_1$-L1, but not *qtr2Δ* (Figure 4B), showing that the presence of Q-L1 in tRNA *in vivo* depended on functional TGT. As in bacteria, preQ$_1$-L1 did not negatively affect cell growth (Supplementary Figure S4c), and no labelling was observed with preQ$_1$-L2 and -L3, again indicating that their derivatives are not bioavailable for incorporation into tRNAs *in vivo*.

Collectively, the above experiments indicate that preQ$_1$-L1 can readily be employed as a proxy for Q from the perspective of synthetic biology. To further develop this compound for the investigation of the epitranscriptome, we made use of the click chemistry feature of preQ$_1$-L1 to identify RNAs into which it was incorporated *in vivo* by eTGT.

For this purpose, total RNA isolated from *S. pombe* wild-type or *qtr2Δ* cells that were cultured in the presence of preQ$_1$-L1 was bio-conjugated *in vitro* with alkyne-functionalized biotin. Subsequent to affinity purification using streptavidin-coated magnetic beads, the biotin-labelled RNA was subjected to reverse transcription and high-throughput sequencing (Figure 5A, termed Q-RIP-Seq). The analysis showed that the known cytosolic Q-tRNAs tRNA$^{Asn}$, tRNA$^{Asp}$, tRNA$^{His}$ and tRNA$^{Tyr}$ were significantly enriched from WT, but not *qtr2Δ* cells ($n = 3$, $P_{adj} < 0.1$, Figure 5B, C and Supplementary Figure S5). Other enriched signals from snoR38 and snoR69 were scrutinised as potential substrates of TGT-mediated incorporation of preQ$_1$-L1. However, neither APB Northern blotting nor quantification by q-RT-PCR substantiated this hypothesis (Supplementary Figure S6). Interestingly, mitochondrial tRNA$^{Asn}$, when analysed for q content by APB-northern blot, was queuosinylated to about 50% (Supplementary Figure S5b). The fact that no mitochondrial tRNA sequences were found in Q-RIP-Seq could mean that they are too low in abundance. An alternative explanation would be that preQ$_1$-L1 is not incorporated into mitochondrial tRNA. The above findings indicate that the four known Q-tRNAs are the only cytosolic RNAs that are Q-modified in *S. pombe*, which is congruent with crosslinking-based studies in human cells (41). These results establish that any major metabolic influence resulting from feeding preQ$_1$-L1 would be mediated through the four classical tRNA substrates of TGT. It should, however, be noted that an early study reported preQ1-modification *in vitro* of larger RNA species in *E. coli* (63).

### *In vivo* interactions of synthetic preQ$_1$ analogues in eukaryotes

Having established that preQ$_1$-L1 is actively incorporated into native tRNAs, we next investigated a particularly interesting effect of queuosine, namely a so-called tRNA modification circuit, where the formation of one modification is enhanced by the presence of another modification (64). The particular circuit involving queuosine was first identified in *S. pombe*. We had shown earlier by RNA bisulfite sequencing that the formation of m$^5$C38 in tRNA$^{Asp}$ by the Dnmt2 tRNA methyltransferase is strongly enhanced by the presence of queuosine at position 34 (Figure 6A) (38,49).

We therefore asked whether Q-L1 can serve as a biologically active surrogate for queuosine in this circuit. Figure 6B shows the m$^5$C38 levels of tRNA$^{Asp}$ in response to increasing concentrations of preQ$_1$-L1 in medium otherwise free of queuosine derivatives. A clear dose-dependent increase of the C38 methylation level was observed, indicating that the incorporated preQ$_1$-L1 is functionally integrated into this modification circuit, efficiently replacing queuosine in its capability of triggering Dnmt2 activity in *S. pombe*. Considering the direct functional connection of Q/Q-L1 and m$^5$C38, the increase of the C38 methylation level from 15% in non-treated culture up to 60% in cultures supplemented with 100 nm preQ$_1$-L1 points to its incorporation in significant amounts in *S. pombe*. However, it is important to mention that the effect of preQ$_1$-L1 incorporation on tRNA$^{Asp}$ methylation is less efficient compared to the known effect of Q under

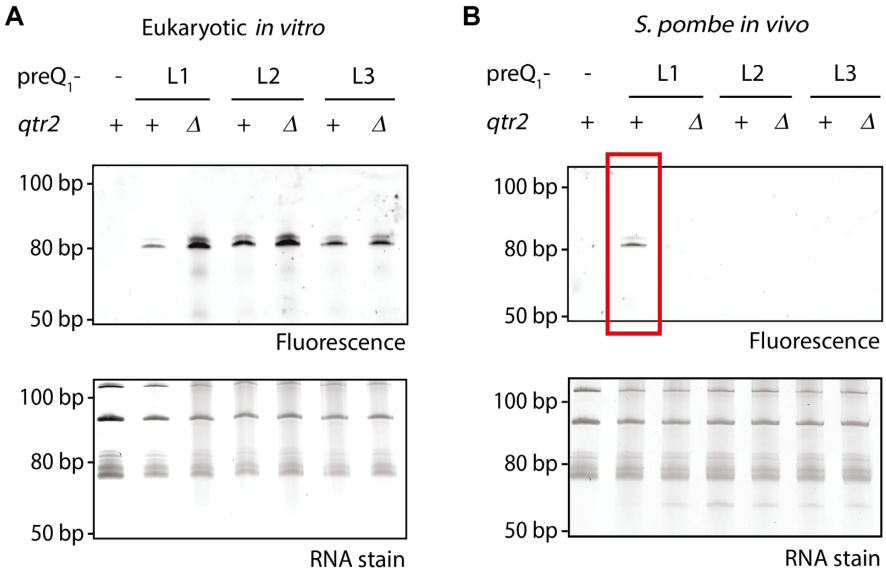


**Figure 4.** *In vitro* and *in vivo* incorporation of preQ$_1$-ligands in *S. pombe* tRNA. (**A**) Analysis of the total RNA click product after human tRNA guanine transglycosylase (hTGT)-catalysed incorporation of preQ$_1$-ligands L1–L3 into RNA from *S. pombe* by denaturing PAGE and visualization by fluorescence scan for AlexaFluor 594 (excitation: 532 nm, emission: 610 nm). Total RNA was extracted from *S. pombe* WT cells containing functional TGT (+) and *qtr2Δ* cells that lack functional TGT (*Δ*), which were both cultured in the presence of queuine. The incubation of total RNA from WT cells without preQ$_1$-ligand (-) served as a negative control. A loading control was obtained by RNA staining with SybrGold. (**B**) Analysis of total tRNA from *S. pombe* WT (+) and *qtr2Δ* (*Δ*) cells that were cultured in the presence of 0.1 μM of the respective preQ$_1$-ligand after click reaction by denaturing PAGE and subsequent visualization as described above. Total RNA from *S. pombe* WT cells supplemented with 0.1 μM queuine (–) instead of preQ$_1$-ligands was used as a negative control.

normal conditions, as we previously reported (38). The incorporation efficiency in *E. coli* can only be gauged even more indirectly, namely by comparison of fluorescent signals after click (Supplementary Figure S4d).

Lastly, we were also able to demonstrate successful incorporation of preQ$_1$-L1 in HeLa human cells deprived of q (Supplementary Figure S7a). In analogy to the earlier presented analysis of *E. coli* polysomes, we also investigated the levels of Q-L1 in tRNA purified from F0 and F3 of accordingly treated HeLa cultures. Similar to our observations in *E. coli*, the amount of Q-L1 detected in the polysomal tRNA (F3 fraction) from preQ$_1$-L1 fed HeLa cells was comparable to its level in the respective F0 fraction, indicating that Q-L1-containing tRNAs actively engage in protein biosynthesis *in cellulo* (Supplementary Figure S7b). This result indicates relevance of our investigations with respect to biomedical considerations, e.g. potential therapeutic interventions.

## DISCUSSION

Interest in concepts for the incorporation of modified and/or non-natural derivatives of metabolites into nucleic acids has been steadily increasing, boosted in part by a surge in RNA modification research, and, more recently, in mRNA-based vaccines. Post-synthetic derivatization of RNA *in vitro*, e.g. by methyltransferases has been exploited for labelling in conjunction with click chemistry (65–69). In the queuosine field, a number of q-derived compounds, including clickable tetrazine derivatives, have been incorporated into native RNA preparation *in vitro* using recombinant TGT, and applied to fluorescent labelling, affinity purification, and interactome research (42–44,70,71). In a previous study, Brooks *et al.* reported that azide congeners of preQ$_1$ lacking the methylene amine were not incorporated by the TGT which they traced to the necessity of this structural element for a successful binding to the enzyme forming hydrogen bonds between aminoacid residues Leu231 and Met260 of the enzyme (72,73). Although, as mentioned, strong indirect evidence (34) suggested that incorporation of nonnatural q derivatives should be feasible in principle, no *in vivo* labelling of Q-tRNAs with clickable q-derivatives has been demonstrated so far.

Overall, concepts and applications in the RNA field currently move from *in vitro* (74) to metabolic feeding approaches *in cellulo* and *in vivo*. Here, the use of noncanonical nucleoside structures has opened up new experimental avenues in the community. As an example, in RNA modification research feeding of methionine analogues featuring e.g. propargyl residues, has enabled their incorporation into RNA *in lieu* of methyl groups. Subsequent derivatization by click chemistry was exploited for determination of modification sites (75,76,66).

An important progress featured in our work is that we demonstrate low toxicity of the labelling compound and provide corresponding data at the molecular level. Elsewhere in the field, little attention is paid to the physiological impact of surrogate feeding. In most cases, a moderate survival rate in cell culture is sufficient to conduct e.g. -omics type analyses after incorporation (75–77). However, in the next steps of its development, the field might conceivably move to applications in model organisms. Here, by the latest, one will need

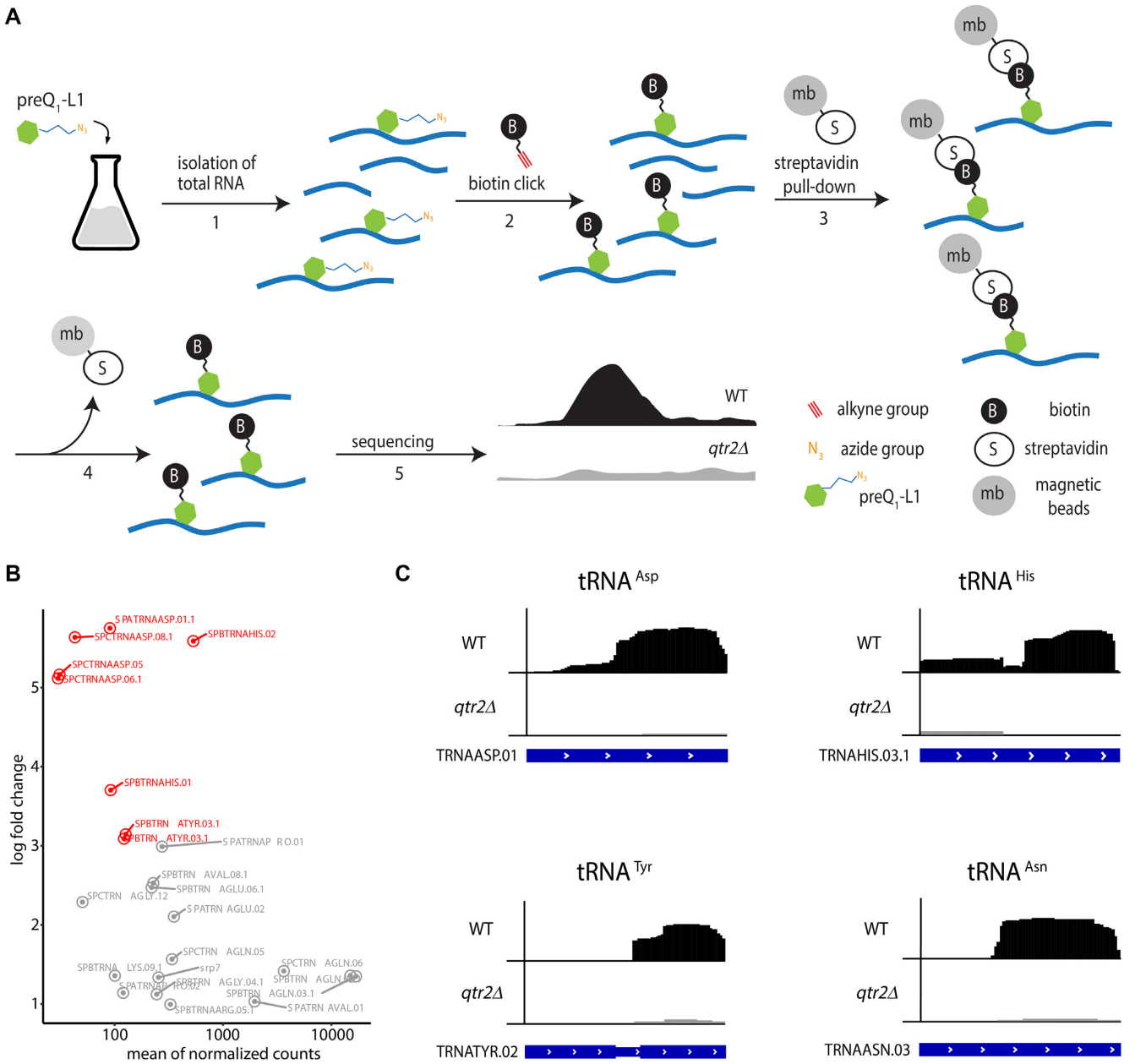


**Figure 5.** *In vivo* identification of Q-modified RNAs in *S. pombe* based on metabolic labelling with preQ$_1$-L1 and high-throughput sequencing (Q-RIP-Seq). (**A**) Concept of metabolic labelling and immunoprecipitation of Q-modified RNAs. *S. pombe* was cultured in the presence of 0.1 μM preQ$_1$-L1, leading to incorporation into otherwise Q-modified RNAs. Total RNA was extracted (1) and bio-conjugated *in vitro* with alkyne-functionalized biotin (2). Biotin-labelled RNAs were subsequently affinity-purified using streptavidin-coated magnetic beads (3), reverse-transcribed and subjected to high-throughput sequencing (5). As a control, metabolic labelling was performed in an *S. pombe* strain lacking TGT (*qtr2Δ*). (**B**) Log2 fold change of normalized read counts of RNAs from WT compared to *qtr2Δ* determined by exomePeak2. Red: tRNA$^{Asp}$, tRNA$^{His}$ and tRNA$^{Tyr}$; (three independent replicates). (**C**) Q-RIP-Seq of tRNA$^{Asp}$, tRNA$^{His}$, tRNA$^{Tyr}$ and tRNA$^{Asn}$ after metabolic labelling with preQ$_1$-L1 in *S. pombe* WT and *qtr2Δ* cells. Coverage of the tRNA sequences from modified (WT, black) and unmodified (*qtr2Δ*, grey) samples is shown. The transcript architecture is shown below with thin and thick parts representing introns and mature tRNA sequences. Replicate 1 of three independent experiments is shown. Plots were generated using IGV.

to adopt concepts from medicinal chemistry, such as cell permeability, and toxicity. In this respect, the work presented here pioneers the combination of metabolic feeding of clickable surrogates with investigations into their physiological molecular impact after cellular uptake and their usage for the enrichment and identification of RNA species that were labelled *in vivo* by endogenous TGT. Apart from the observation of growth inhibition of q derivatives in eukaryotic cell culture, which are somewhat suggestive (78), there is strong indirect evidence for the actual incorporation of a q-derivative by TGT *in vivo* in mouse (34), however without direct analysis of the tRNA. Significantly, said case features a background of medicinal chemistry, and the compound used is structurally related to our preQ1-L series used here. It does, however, feature a lipophilic phenylpropyl sidechain which is likely causative

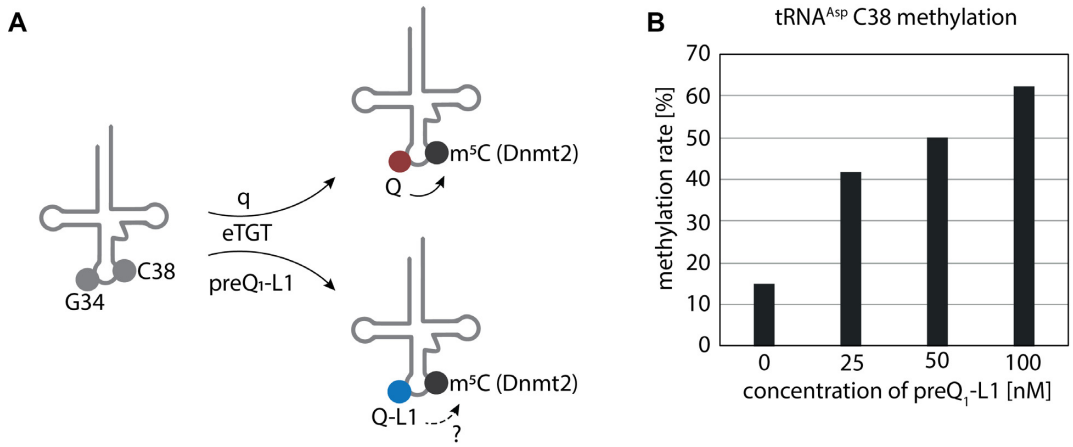


**Figure 6.** Incorporation of $preQ_1$-L1 in $tRNA^{Asp}$ in *S. pombe* stimulates C38 methylation by Dnmt2. (**A**) Incorporation of q or $preQ_1$-L1 by eukaryotic tRNA guanine transglycosylase (eTGT) affects Dnmt2 activity in *S. pombe* (Pmt1). (**B**) Determination of $tRNA^{Asp}$ methylation levels at C38 in total RNA from *S. pombe* WT supplemented with the indicated concentrations of $preQ_1$-L1 by RNA bisulfite sequencing combined with high throughput sequencing.

of, or enhancing the compound's cell permeability and biodistribution.

In the present work, we have developed the azido-propyl-derivative $preQ_1$-L1 as a bioactive surrogate for $preQ_1$ *in vivo*. $preQ_1$-L1 is taken up into unicellular prokaryotes as well as into eukaryotes, and incorporated into the known tRNA substrates of TGT. The resulting nucleoside is semi-synthetic in that its sugar moiety is native, while its nucleobase is synthetic. Its azide moiety can be employed to metabolically label and isolate Q-modified RNAs by affinity purification after conjugation by click chemistry. We used this feature to confirm similar data from human cells, obtained after UV-crosslinking (41). Taken together, this means that the single most important molecular interaction for a physiological impact of q (or $preQ_1$-L1) is mediated through position 34 in the anticodons of the four known TGT substrate tRNAs.

Known molecular interactions issuing from this nucleobase are mostly restricted to tRNA aminoacylation and mRNA decoding, which we have interrogated by investigating the amount of Q-L1 carrying tRNAs on polysomes. While Q-L1 was less abundant there than was native Q, it was clearly present, featuring an equal distribution between actively translating tRNAs and the cytoplasmic pool in both bacterial and human cell preparations.

One other known effect of Q was also faithfully emulated by Q-L1, namely the stimulation of $m^5C38$ formation by Dnmt2 in the anticodon stem of $tRNA^{Asp}$, representing a so-called modification loop. Technically speaking, we report the first-ever manipulation of a modification loop by atomic mutagenesis *in vivo*.

In spite of numerous described Q-dependent implications in various diseases, starting from cancer (29–32) to neurological and neuropsychiatric disorders, such as multiple sclerosis, schizophrenia and Parkinson (79,80,33,34), a defined mechanism explaining the role of Q in these pathologies is still missing (28). Recently, we discovered a direct connection between Q, accuracy and the speed of codon-biased translation (27,28), which promotes protein folding and prevents the accumulation of misfolded proteins. The fact that Q-L1 is functionally involved in the translational process in a 'minimally invasive' system, opens the possibility to study the roles of Q34 modifications in protein translation in normal and pathogenic human cell lines, directly combining click chemistry or LC–MS/MS with polysome profiling.

In summary, the combination of very few queuosinylation sites and the effective functional replacement of Q by Q-L1 on the molecular level, makes the q/Q system uniquely suited for a 'minimally invasive' placement of a non-natural nucleobase within the total cellular RNA.

## DATA AVAILABILITY

HTS data for Q-RIP-Seq experiments are available in the NCBI GEO database, record GSE210404. All data needed to evaluate the conclusions in the paper are present in the paper and/or Supplementary Data. Additional data related to this paper may be requested from the authors.

## SUPPLEMENTARY DATA

Supplementary Data are available at NAR Online.

## ACKNOWLEDGEMENTS

Eva Neuner (Innsbruck) is thanked for discussions.
*Author contributions*: A.E.E.-M. and M.H. conceived and supervised the project. L.B., N.K. and L.V. performed the majority of the experimental work. These authors contributed equally and are listed in alphabetical order. L.F. and R.M. provided $preQ_1$-L1-3. F.T. performed HeLa culture and polysome preparations. C.S. and M.W. helped with *E. coli* polysome preparations. All authors discussed the results. L.B., M.H. and L.V. wrote the manuscript with input from all the other authors.

## FUNDING

Deutsche Forschungsgemeinschaft (DFG, German Research Foundation) [TRR-319 TP C03, SPP1784, HE

3397/13-2, HE 3397/14-2 to M.H., TRR-319 TP A06 to F.T., TRR-319 TP B05 to M.-L.W.]; [DFG SPP1784 to A.E.E.-M.]; R.M. was supported by the Austrian Science Fund FWF [P31691 and F8011-B]. Funding for open access charge: Johannes Gutenberg University.

*Conflict of interest statement.* M.H. is a consultant for Moderna Inc. The other authors declare that they have no competing interests.

## REFERENCES


1. El Yacoubi,B., Bailly,M. and de Crécy-Lagard,V. (2012) Biosynthesis and function of posttranscriptional modifications of transfer RNAs. *Annu. Rev. Genet.*, **46**, 69–95.
2. Lorenz,C., Lünse,C.E. and Mörl,M. (2017) tRNA modifications: impact on structure and thermal adaptation. *Biomolecules*, **7**, 35.
3. Motorin,Y. and Helm,M. (2010) tRNA stabilization by modified nucleotides. *Biochemistry*, **49**, 4934–4944.
4. Boccaletto,P., Stefaniak,F., Ray,A., Cappannini,A., Mukherjee,S., Purta,E., Kurkowska,M., Shirvanizadeh,N., Destefanis,E., Groza,P. *et al.* (2022) MODOMICS: a database of RNA modification pathways. 2021 update. *Nucleic Acids Res.*, **50**, D231–D235.
5. Fergus,C., Barnes,D., Alqasem,M.A. and Kelly,V.P. (2015) The queuine micronutrient: charting a course from microbe to man. *Nutrients*, **7**, 2897–2929.
6. Harada,F. and Nishimura,S. (1972) Possible anticodon sequences of tRNA his tRNA asm and tRNA asp from escherichia coli b. Universal presence of nucleoside q in the first postion of the anticondons of these transfer ribonucleic acids. *Biochemistry*, **11**, 301–308.
7. Kasai,H., Oashi,Z., Harada,F., Nishimura,S., Oppenheimer,N.J., Crain,P.F., Liehr,J.G., Minden,D.L.von and McCloskey,J.A. (1975) Structure of the modified nucleoside q isolated from escherichia coli transfer ribonucleic acid. 7-(4,5-cis-Dihydroxy-1-cyclopenten-3-ylaminomethyl)-7-deazaguanosine. *Biochemistry*, **14**, 4198–4208.
8. Phillips,G., El Yacoubi,B., Lyons,B., Alvarez,S., Iwata-Reuyl,D. and Crécy-Lagard,V.de (2008) Biosynthesis of 7-deazaguanosine-modified tRNA nucleosides: a new role for GTP cyclohydrolase I. *J. Bacteriol.*, **190**, 7876–7884.
9. McCarty,R.M., Somogyi,A. and Bandarian,V. (2009) Escherichia coli QueD is a 6-carboxy-5,6,7,8-tetrahydropterin synthase. *Biochemistry*, **48**, 2301–2303.
10. McCarty,R.M., Somogyi,A., Lin,G., Jacobsen,N.E. and Bandarian,V. (2009) The deazapurine biosynthetic pathway revealed: in vitro enzymatic synthesis of preq(0) from guanosine 5'-triphosphate in four steps. *Biochemistry*, **48**, 3847–3852.
11. van Lanen,S.G., Reader,J.S., Swairjo,M.A., Crécy-Lagard,V.de, Lee,B. and Iwata-Reuyl,D. (2005) From cyclohydrolase to oxidoreductase: discovery of nitrile reductase activity in a common fold. *Proc. Nat. Acad. Sci. U.S.A.*, **102**, 4264–4269.
12. Okada,N. and Nishimura,S. (1979) Isolation and characterization of a guanine insertion enzyme, a specific tRNA transglycosylase, from escherichia coli. *J. Biol. Chem.*, **254**, 3061–3066.
13. Okada,N., Noguchi,S., Kasai,H., Shindo-Okada,N., Ohgi,T., Goto,T. and Nishimura,S. (1979) Novel mechanism of post-transcriptional modification of tRNA. Insertion of bases of q precursors into tRNA by a specific tRNA transglycosylase reaction. *J. Biol. Chem.*, **254**, 3067–3073.
14. Slany,R.K., Bösl,M. and Kersten,H. (1994) Transfer and isomerization of the ribose moiety of adomet during the biosynthesis of queuosine tRNAs, a new unique reaction catalyzed by the QueA protein from escherichia coli. *Biochimie*, **76**, 389–393.
15. Miles,Z.D., McCarty,R.M., Molnar,G. and Bandarian,V. (2011) Discovery of epoxyqueuosine (oQ) reductase reveals parallels between halorespiration and tRNA modification. *Proc. Nat. Acad. Sci. U.S.A.*, **108**, 7368–7372.
16. Patel,B.I., Heiss,M., Samel-Pommerencke,A., Carell,T. and Ehrenhofer-Murray,A.E. (2022) Queuosine salvage in fission yeast by Qng1-mediated hydrolysis to queuine. *Biochem. Biophys. Res. Commun.*, **624**, 146–150.
17. Farkas,W.R., Jacobson,K.B. and Katze,J.R. (1984) Substrate and inhibitor specificity of tRNA-guanine ribosyltransferase. *Biochim. Biophys. Acta*, **781**, 64–75.
18. Boland,C., Hayes,P., Santa-Maria,I., Nishimura,S. and Kelly,V.P. (2009) Queuosine formation in eukaryotic tRNA occurs via a mitochondria-localized heteromeric transglycosylase. *J. Biol. Chem.*, **284**, 18218–18227.
19. Chen,Y.-C., Kelly,V.P., Stachura,S.V. and Garcia,G.A. (2010) Characterization of the human tRNA-guanine transglycosylase: confirmation of the heterodimeric subunit structure. *RNA*, **16**, 958–968.
20. Johannsson,S., Neumann,P. and Ficner,R. (2018) Crystal structure of the human tRNA guanine transglycosylase catalytic subunit QTRT1. *Biomolecules*, **8**, 81.
21. Grosjean,H. and Westhof,E. (2016) An integrated, structure- and energy-based view of the genetic code. *Nucleic Acids Res.*, **44**, 8020–8040.
22. Morris,R.C., Brown,K.G. and Elliott,M.S. (1999) The effect of queuosine on tRNA structure and function. *J. Biomol. Struct. Dyn.*, **16**, 757–774.
23. Noguchi,S., Nishimura,Y., Hirota,Y. and Nishimura,S. (1982) Isolation and characterization of an escherichia coli mutant lacking tRNA-guanine transglycosylase. Function and biosynthesis of queuosine in tRNA. *J. Biol. Chem.*, **257**, 6544–6550.
24. Manickam,N., Joshi,K., Bhatt,M.J. and Farabaugh,P.J. (2016) Effects of tRNA modification on translational accuracy depend on intrinsic codon-anticodon strength. *Nucleic Acids Res.*, **44**, 1871–1881.
25. Meier,F., Suter,B., Grosjean,H., Keith,G. and Kubli,E. (1985) Queuosine modification of the wobble base in tRNAHis influences 'in vivo' decoding properties. *EMBO J.*, **4**, 823–827.
26. Zaborske,J.M., DuMont,V.L.B., Wallace,E.W.J., Pan,T., Aquadro,C.F. and Drummond,D.A. (2014) A nutrient-driven tRNA modification alters translational fidelity and genome-wide protein coding across an animal genus. *PLoS Biol.*, **12**, e1002015.
27. Müller,M., Legrand,C., Tuorto,F., Kelly,V.P., Atlasi,Y., Lyko,F. and Ehrenhofer-Murray,A.E. (2019) Queuine links translational control in eukaryotes to a micronutrient from bacteria. *Nucleic Acids Res.*, **47**, 3711–3727.
28. Tuorto,F., Legrand,C., Cirzi,C., Federico,G., Liebers,R., Müller,M., Ehrenhofer-Murray,A.E., Dittmar,G., Gröne,H.-J. and Lyko,F. (2018) Queuosine-modified tRNAs confer nutritional control of protein translation. *EMBO J.*, **37**, e99777.
29. Zhang,J., Lu,R., Zhang,Y., Matuszek,Ż., Zhang,W., Xia,Y., Pan,T. and Sun,J. (2020) tRNA queuosine modification enzyme modulates the growth and microbiome recruitment to breast tumors. *Cancers*, **12**, 628.
30. Sebastiani,M., Behrens,C., Dörr,S., Gerber,H.-D., Benazza,R., Hernandez-Alba,O., Cianférani,S., Klebe,G., Heine,A. and Reuter,K. (2022) Structural and biochemical investigation of the heterodimeric murine tRNA-Guanine transglycosylase. *ACS Chem. Biol.*, **17**, 2229–2247.
31. Chen,Y.L. and Wu,R.T. (1994) Altered queuine modification of transfer RNA involved in the differentiation of human K562 erythroleukemia cells in the presence of distinct differentiation inducers. *Cancer Res.*, **54**, 2192–2198.
32. Dirheimer,G., Baranowski,W. and Keith,G. (1995) Variations in tRNA modifications, particularly of their queuine content in higher eukaryotes. Its relation to malignancy grading. *Biochimie*, **77**, 99–103.
33. Richard,P., Kozlowski,L., Guillorit,H., Garnier,P., McKnight,N.C., Danchin,A. and Manière,X. (2021) Queuine, a bacterial-derived hypermodified nucleobase, shows protection in in vitro models of neurodegeneration. *PLoS One*, **16**, e0253216.
34. Varghese,S., Cotter,M., Chevot,F., Fergus,C., Cunningham,C., Mills,K.H., Connon,S.J., Southern,J.M. and Kelly,V.P. (2017) In vivo modification of tRNA with an artificial nucleobase leads to full disease remission in an animal model of multiple sclerosis. *Nucleic Acids Res.*, **45**, 2029–2039.
35. Rakovich,T., Boland,C., Bernstein,I., Chikwana,V.M., Iwata-Reuyl,D. and Kelly,V.P. (2011) Queuosine deficiency in eukaryotes compromises tyrosine production through increased tetrahydrobiopterin oxidation. *J. Biol. Chem.*, **286**, 19354–19363.
36. Kulkarni,S., Rubio,M.A.T., Hegedűsová,E., Ross,R.L., Limbach,P.A., Alfonzo,J.D. and Paris,Z. (2021) Preferential import of queuosine-modified tRNAs into trypanosoma brucei

mitochondrion is critical for organellar protein synthesis. *Nucleic Acids Res.*, **49**, 8247–8260.
37. Hurt,J.K., Olgen,S. and Garcia,G.A. (2007) Site-specific modification of shigella flexneri virF mRNA by tRNA-guanine transglycosylase in vitro. *Nucleic Acids Res.*, **35**, 4905–4913.
38. Müller,M., Hartmann,M., Schuster,I., Bender,S., Thüring,K.L., Helm,M., Katze,J.R., Nellen,W., Lyko,F. and Ehrenhofer-Murray,A.E. (2015) Dynamic modulation of Dnmt2-dependent tRNA methylation by the micronutrient queuine. *Nucleic Acids Res.*, **43**, 10952–10962.
39. Ehrenhofer-Murray,A.E. (2017) Cross-Talk between dnmt2-dependent tRNA methylation and queuosine modification. *Biomolecules*, **7**, 14.
40. Johannsson,S., Neumann,P., Wulf,A., Welp,L.M., Gerber,H.-D., Krull,M., Diederichsen,U., Urlaub,H. and Ficner,R. (2018) Structural insights into the stimulation of s. pombe dnmt2 catalytic efficiency by the tRNA nucleoside queuosine. *Sci. Rep.*, **8**, 8880.
41. Fergus,C., Al-Qasem,M., Cotter,M., McDonnell,C.M., Sorrentino,E., Chevot,F., Hokamp,K., Senge,M.O., Southern,J.M., Connon,S.J. *et al.* (2021) The human tRNA-guanine transglycosylase displays promiscuous nucleobase preference but strict tRNA specificity. *Nucleic Acids Res.*, **49**, 4877–4890.
42. Alexander,S.C., Busby,K.N., Cole,C.M., Zhou,C.Y. and Devaraj,N.K. (2015) Site-Specific covalent labeling of RNA by enzymatic transglycosylation. *J. Am. Chem. Soc.*, **137**, 12756–12759.
43. Zhang,D., Zhou,C.Y., Busby,K.N., Alexander,S.C. and Devaraj,N.K. (2018) Light-Activated control of translation by enzymatic covalent mRNA labeling. *Angew. Chem. Int. Ed. Engl.*, **57**, 2822–2826.
44. Ehret,F., Zhou,C.Y., Alexander,S.C., Zhang,D. and Devaraj,N.K. (2018) Site-Specific covalent conjugation of modified mRNA by tRNA guanine transglycosylase. *Mol. Pharmaceutics*, **15**, 737–742.
45. Neuner,E., Frener,M., Lusser,A. and Micura,R. (2018) Superior cellular activities of azido- over amino-functionalized ligands for engineered preQ1 riboswitches in E.coli. *RNA Biol.*, **15**, 1376–1383.
46. Jakobi,S., Nguyen,T.X.P., Debaene,F., Metz,A., Sanglier-Cianférani,S., Reuter,K. and Klebe,G. (2014) Hot-spot analysis to dissect the functional protein-protein interface of a tRNA-modifying enzyme. *Proteins*, **82**, 2713–2732.
47. Gerber,H.-D. and Klebe,G. (2012) Concise and efficient syntheses of preQ1 base, q base, and (ent)-Q base. *Org. Biomol. Chem.*, **10**, 8660–8668.
48. Kraus,A.J., Brink,B.G. and Siegel,T.N. (2019) Efficient and specific oligo-based depletion of rRNA. *Sci. Rep.*, **9**, 12281.
49. Becker,M., Müller,S., Nellen,W., Jurkowski,T.P., Jeltsch,A. and Ehrenhofer-Murray,A.E. (2012) Pmt1, a dnmt2 homolog in *Schizosaccharomyces pombe*, mediates tRNA methylation in response to nutrient signaling. *Nucleic Acids Res.*, **40**, 11648–11658.
50. Schmid,K., Adobes-Vidal,M. and Helm,M. (2017) Alkyne-Functionalized coumarin compound for analytic and preparative 4-thiouridine labeling. *Bioconjug. Chem.*, **28**, 1123–1134.
51. Yuan,Y., Hutinet,G., Valera,J.G., Hu,J., Hillebrand,R., Gustafson,A., Iwata-Reuyl,D., Dedon,P.C. and Crécy-Lagard,V.de (2018) Identification of the minimal bacterial 2'-deoxy-7-amido-7-deazaguanine synthesis machinery. *Mol. Microbiol.*, **110**, 469–483.
52. Morgan,M., Anders,S., Lawrence,M., Aboyoun,P., Pagès,H. and Gentleman,R. (2009) ShortRead: a bioconductor package for input, quality assessment and exploration of high-throughput sequence data. *Bioinformatics*, **25**, 2607–2608.
53. Rohde,C., Zhang,Y., Reinhardt,R. and Jeltsch,A. (2010) BISMA—fast and accurate bisulfite sequencing data analysis of individual clones from unique and repetitive sequences. *BMC Bioinf.*, **11**, 230.
54. Jiang,H., Lei,R., Ding,S.-W. and Zhu,S. (2014) Skewer: a fast and accurate adapter trimmer for next-generation sequencing paired-end reads. *BMC Bioinf.*, **15**, 182.
55. Patro,R., Duggal,G., Love,M.I., Irizarry,R.A. and Kingsford,C. (2017) Salmon provides fast and bias-aware quantification of transcript expression. *Nat. Methods*, **14**, 417–419.
56. Kim,D., Langmead,B. and Salzberg,S.L. (2015) HISAT: a fast spliced aligner with low memory requirements. *Nat. Methods*, **12**, 357–360.
57. Li,H., Handsaker,B., Wysoker,A., Fennell,T., Ruan,J., Homer,N., Marth,G., Abecasis,G. and Durbin,R. (2009) The sequence alignment/map format and SAMtools. *Bioinformatics*, **25**, 2078–2079.
58. Love,M.I., Huber,W. and Anders,S. (2014) Moderated estimation of fold change and dispersion for RNA-seq data with DESeq2. *Genome Biol.*, **15**, 550.
59. Ignatiadis,N., Klaus,B., Zaugg,J.B. and Huber,W. (2016) Data-driven hypothesis weighting increases detection power in genome-scale multiple testing. *Nat. Methods*, **13**, 577–580.
60. Ignatiadis,N. and Huber,W. (2021) Covariate powered cross-weighted multiple testing. *J. R. Stat. Soc. Series B*, **83**, 720–751.
61. Meng,J., Cui,X., Rao,M.K., Chen,Y. and Huang,Y. (2013) Exome-based analysis for RNA epigenome sequencing data. *Bioinformatics*, **29**, 1565–1567.
62. Robinson,J.T., Thorvaldsdóttir,H., Winckler,W., Guttman,M., Lander,E.S., Getz,G. and Mesirov,J.P. (2011) Integrative genomics viewer. *Nat. Biotechnol.*, **29**, 24–26.
63. Brooks,A.F., Vélez-Martínez,C.S., Showalter,H.D.H. and Garcia,G.A. (2012) Investigating the prevalence of queuine in escherichia coli RNA via incorporation of the tritium-labeled precursor, preQ(1). *Biochem. Biophys. Res. Commun.*, **425**, 83–88.
64. Motorin,Y. and Helm,M. (2022) RNA nucleotide methylation: 2021 update, wiley interdisciplinary reviews. *RNA*. **15**, 2021.
65. Motorin,Y., Burhenne,J., Teimer,R., Koynov,K., Willnow,S., Weinhold,E. and Helm,M. (2011) Expanding the chemical scope of RNA:methyltransferases to site-specific alkynylation of RNA for click labeling. *Nucleic Acids Res.*, **39**, 1943–1952.
66. Fischer,T.R., Meidner,L., Schwickert,M., Weber,M., Zimmermann,R.A., Kersten,C., Schirmeister,T. and Helm,M. (2022) Chemical biology and medicinal chemistry of RNA methyltransferases. *Nucleic Acids Res.*, **50**, 4216–4245.
67. Schulz,D., Holstein,J.M. and Rentmeister,A. (2013) A chemo-enzymatic approach for site-specific modification of the RNA cap. *Angew. Chem. Int. Ed. Engl.*, **52**, 7874–7878.
68. Muttach,F. and Rentmeister,A. (2016) A biocatalytic cascade for versatile one-pot modification of mRNA starting from methionine analogues. *Angew. Chem. Int. Ed. Engl.*, **55**, 1917–1920.
69. Ovcharenko,A., Weissenboeck,F.P. and Rentmeister,A. (2021) Tag-Free internal RNA labeling and photocaging based on mRNA methyltransferases. *Angew. Chem. (Int. Ed. Engl.)*, **60**, 4098–4103.
70. Busby,K.N., Fulzele,A., Zhang,D., Bennett,E.J. and Devaraj,N.K. (2020) Enzymatic RNA biotinylation for affinity purification and identification of RNA-Protein interactions. *ACS Chem. Biol.*, **15**, 2247–2258.
71. Zhou,C.Y., Alexander,S.C. and Devaraj,N.K. (2017) Fluorescent turn-on probes for wash-free mRNA imaging via covalent site-specific enzymatic labeling. *Chem. Sci.*, **8**, 7169–7173.
72. Brooks,A.F., Garcia,G.A. and Showalter,H.D. (2021) Synthesis of azide congeners of preQ 1 as potential substrates for tRNA guanine transglycosylase. *J Heterocyclic Chem*, **58**, 1192–1198.
73. Xie,W., Liu,X. and Huang,R.H. (2003) Chemical trapping and crystal structure of a catalytic tRNA guanine transglycosylase covalent intermediate. *Nat. Struct. Biol.*, **10**, 781–788.
74. Croce,S., Serdjukow,S., Carell,T. and Frischmuth,T. (2020) Chemoenzymatic preparation of functional click-labeled messenger RNA. *Chembiochem*, **21**, 1641–1646.
75. Hartstock,K., Nilges,B.S., Ovcharenko,A., Cornelissen,N.V., Püllen,N., Lawrence-Dörner,A.-M., Leidel,S.A. and Rentmeister,A. (2018) Enzymatic or in vivo installation of propargyl groups in combination with click chemistry for the enrichment and detection of methyltransferase target sites in RNA. *Angew. Chem. (Int. Ed. Engl.)*, **57**, 6342–6346.
76. Hartstock,K., Ovcharenko,A., Kueck,N.A., Spacek,P., Cornelissen,N.V., Hüwel,S., Dieterich,C. and Rentmeister,A. (2022) MePMe-seq: Antibody-free simultaneous m6A and m5C mapping in mRNA by metabolic propargyl labeling and sequencing. bioRxiv doi: https://doi.org/10.1101/2022.03.16.484494, 16 March 2022, preprint: not peer reviewed.
77. Shu,X., Cao,J., Cheng,M., Xiang,S., Gao,M., Li,T., Ying,X., Wang,F., Yue,Y., Lu,Z. *et al.* (2020) A metabolic labeling method detects m6A transcriptome-wide at single base resolution. *Nat. Chem. Biol.*, **16**, 887–895.
78. Akimoto,H., Nomura,H., Yoshida,M., Shindo-Okada,N., Hoshi,A. and Nishimura,S. (1986) Queuine analogues. Their synthesis and

inhibition of growth of mouse L5178Y cells in vitro. *J. Med. Chem.*, **29**, 1749–1753.
79. Bednářová,A., Hanna,M., Durham,I., VanCleave,T., England,A., Chaudhuri,A. and Krishnan,N. (2017) Lost in translation: defects in transfer RNA modifications and neurological disorders. *Front. Mol. Neurosci.*, **10**, 135.
80. Skolnick,S.D. and Greig,N.H. (2019) Microbes and monoamines: potential neuropsychiatric consequences of dysbiosis. *Trends Neurosci.*, **42**, 151–163.